Differential Tooth Surface Modification Method for Reducing Vibration in Spiral Bevel and Hypoid Gears

Yu Zhang[1] ✉ – Chengyu Duan[1] – Xiao Li[1] – Zhiyong Wang[1] – Yanli Ma[1] – Guoqi He[2]

1 Institute of Modern Mechanical Transmission Engineering Technology, Central South University of Forestry and Technology, China

2 School of Mechanical Engineering, Hunan University of Technology, China

✉ zhyu@csuft.edu.cn

Abstract *To address the issue of increased gear noise in electric vehicle drivetrains due to higher rotational speeds, a differential tooth surface modification method for spiral bevel and hypoid gears is proposed. A mathematical model for spiral bevel and hypoid gears is established using the vector method. Based on this model, a finite element dynamic model of the gears is developed through secondary development using Adams software. A tooth surface modification approach involving parameters (bias factor and profile separation factor) varying according to a sinusoidal function is investigated, alongside its impact on micro-topography of the tooth surface. A comparative simulation analysis is performed to evaluate the sinusoidal parameter design method against traditional modification methods, emphasizing gear angular acceleration and meshing force under various operating conditions. The results demonstrate that the differential modification method achieves a significant reduction in the first three orders of meshing frequencies under almost all conditions, with maximum reductions in the first-order frequency amplitudes of the gear angular acceleration and meshing force reaching 22.98 % and 36.05 %, respectively. This confirms the method effectiveness in reducing gear vibration and noise. The proposed differential modification method for spiral bevel and hypoid gears offers a novel approach for vibration and noise mitigation, offering valuable technical support for designing and manufacturing of high-performance electric vehicles.*

Keywords *spiral bevel and hypoid gears, differential tooth surface modification, dynamic simulation, angular acceleration, meshing force*

Highlights

- *A differential tooth surface modification method is proposed for spiral bevel and hypoid gears.*
- *Sinusoidal design method for modification parameters reduces angular acceleration and meshing force.*
- *1st order spectra of meshing force and angular acceleration drop by 22.98 % and 36.05 %, respectively.*

1 INTRODUCTION

The gear transmission system is one of the main sources of vibration and noise in vehicles. Spiral bevel and hypoid gears are core components in the reducer assembly of electric vehicles (EV), and their transmission performance directly affects the driving experience of the entire vehicle [1,2]. Electrification is currently the dominant trend in automotive development, and EV reducer assemblies are evolving towards higher speeds, increased efficiency, and greater peak torque. Their maximum input speed has reached 30,000 rpm or higher, which is approximately 3 to 10 times higher than those of traditional vehicles with internal combustion engines [3,4]. At high rotation speeds, the gear transmission system's noise has emerged as a dominant noise source in EVs. Unlike internal combustion engine vehicles, EVs lack engine noise to mask other components' sounds. This absence amplifies the perceptibility of reducer assembly noise, which result in reduced acoustic quality compared to conventional vehicles, significantly degrading the noise, vibration, and harshness (NVH) performance of EVs. Existing methods for tooth surface modification of spiral bevel and hypoid gears typically apply the same set of modification parameters (MP) to all tooth surfaces on the same side of a gear, meaning each tooth surface receives a uniform modification amount. Although these traditional tooth surface modification methods are widely adopted, their effectiveness in reducing vibration and noise under high-speed conditions is often unsatisfactory. Cattanei et al. [5] addressed the issue of rotor noise in high-speed motors by systematically varying the spacing between circumferential blades, introducing sidebands to disperse harmonic peak energy, thereby reducing the harmonic peak of blade impact frequency and achieving noise reduction for the rotor. Although the mechanisms of rotor noise and gear noise generation differ significantly, the approach proposed by Cattanei et al. [5] offers new insights into reducing vibration and noise reduction in spiral bevel and hypoid gears.

Vibration and noise reduction are constant themes in gear design, and improving gear transmission performance through tooth surface modification is the most common method [6-8]. Spiral bevel and hypoid gears mainly achieve tooth surface modification by adjusting machine setting parameters and cutter parameters. Mu et al. [9-11] proposed a high-order tooth surface modification method and a function-oriented design method for spiral bevel gears with high-order transmission errors and high contact ratios, aiming to reduce vibration excitation in gear transmission systems. Samani et al. [12] used an innovative tooth surface modification method to study the vibration of nonlinear spiral bevel gears, exploring a new nonlinear vibration analysis method and designing spiral bevel gears with high-order transmission errors. Chen et al. [13] proposed a polynomial ease-off topology modification (PETM) method for the vibration analysis of spiral bevel gears, aiming to minimize the normal meshing force and normal relative displacement to reduce vibration noise. Nie et al. [14] proposed a tooth surface mismatch correction method to eliminate the howling noise of hypoid gears in drive axles during high-speed operation. Lin [15] minimized transmission error by optimizing gear profile modification parameters and adjusting system dynamic parameters, thereby reducing gear whine noise and vibration in automotive axles. Chen et al. [16] employed an active design approach by nonlinearly adjusting machine tool processing parameters for hypoid gears, thereby reducing the vibration and noise of hypoid gears manufactured using the duplex helical method.

In addition to tooth surface modification techniques, optimizing the geometric parameters of gears and the structural parameters of gearboxes, as well as improving manufacturing precision, are also common methods for reducing vibration and noise in spiral bevel and hypoid gears [17,18]. Cai et al. [19] proposed a comprehensive dynamic parameter model to capture the impact of microstructural changes on gear dynamics. Lin et al. [20] investigated the effects of apex error and tilt error on the tooth surface contact trajectory of double-arc spiral bevel gears used to drive the joint axes of industrial robots. Zhu et al. [21] developed a coupled dynamic model consisting of the spiral bevel gear, inclined tail shaft, and laminated membrane in gearboxes, analyzing the impact of membrane coupling and key parameters on the system dynamics. Sun et al. [22] developed a computational model for the carburizing, quenching, and low-temperature tempering processes of face-knurled hypoid gears, to optimize process parameters and reduce heat treatment distortion. Bozca [23,24] achieved a 10 % reduction in the calculated gear whine noise level by optimizing the geometric parameters of the gearbox. Qi [25] proposed a rib layout optimization method that effectively reduces the radiated noise of gearboxes. Anuradha et al. [26] studied the impact of geometric design parameters on the dynamic characteristics of spiral bevel gear sets under different boundary conditions.

Methods such as tooth profile modification and optimization of geometric and structural parameters have been proven effective in reducing vibration and noise in gears. However, with the continuous advancement of EV technology, the demands placed upon gear transmission systems are increasing, and existing vibration and noise reduction techniques are encountering performance bottlenecks. Traditional tooth surface modification methods, which modify all gear teeth with the same surface profile, sometimes fail to achieve the desired noise reduction.

Inspired by Cattanei's concept of differentiated blade spacing design, a novel approach is proposed: varying the modification amount across the teeth of spiral bevel and hypoid gears according to a specific pattern (e.g., a sine curve), creating a differentiated design for each tooth's surface profile. This approach aims to achieve vibration and noise reduction through controlled variation during gear rotation. Differentiated design of tooth flank microstructures enables precise regulation of vibration and noise characteristics. Specifically, introducing additional low-frequency sidebands reduces meshing harmonic amplitudes, thereby achieving noise suppression. Psychoacoustic theory indicates that such low-frequency components enhance auditory masking effects, which significantly decreases meshing harmonic amplitudes and reduces noise annoyance [27].

To validate this new design method, a mathematical model for tooth surface modification was developed, in which the bias factor and profile separation factor of spiral bevel and hypoid gears vary according to a sine function. Simulations of dynamic characteristics such as centroid angular acceleration and meshing force were conducted using Adams software. The dynamic transmission performance of gear pairs using traditional modification (TM) was compared with those with differentiated modification. The results demonstrated that the differentiated modification method significantly enhances the dynamic transmission performance of gear pairs, effectively reducing vibration and noise. This provides a new approach for vibration and noise reduction in spiral bevel and hypoid gears, fundamentally transcending the limitations of conventional tooth surface modification techniques, and representing a paradigm shift from traditional practices employing uniform surface topography across all gear teeth.

2 METHODS AND MATERIALS

2.1 Mathematical Model for Tooth Cutting of Spiral Bevel and Hypoid Gears

The machining principles of spiral bevel and hypoid gears are explained based on mechanical bevel gear machining equipment. The machine's cradle, cutter tilt, and cutter rotation mechanisms are simulated as an imaginary generating gear, where the cutting surface of the cutter head represents a tooth of the generating gear. When the workpiece and the generating gear rotate around their respective axes at a certain transmission ratio, it resembles the meshing transmission of a pair of spiral bevel and hypoid gears, thus completing the tooth machining. This machining method is known as the generating method, and it is generally used for machining pinions. To reduce machining costs, gears typically use a simpler forming method, wherein the gear tooth surface replicates the cutter's cutting surface, simplifying the machine structure by eliminating the cradle, cutter tilt, and cutter rotation mechanisms.. The machining coordinate system for the pinion is shown in Fig. 1. The coordinate system $S_m\{X_m, Y_m, Z_m\}$ is rigidly fixed to the machine, with its origin O_m coinciding with the machine center, and the machine's cradle rotates around the Z_m axis. The coordinate system $S_n\{X_n, Y_n, Z_n\}$ is rigidly fixed to the cradle, with q used to describe the cradle's rotation angle. The coordinate system $S_t\{X_t, Y_t, Z_t\}$ is rigidly fixed to the cutter head, with the origin coinciding with the cutter head center O_t, and the cutter head rotates around the Z_t axis, with θ used to describe the cutter head's rotation angle. The coordinate system $S_j\{X_j, Y_j, Z_j\}$ is used to describe the cutter swivel angle j and radial distance S_r. The coordinate system $S_i\{X_i, Y_i, Z_i\}$ is used to describe the cutter tilt angle i. The coordinate system $S_k\{X_k, Y_k, Z_k\}$ is used to describe the work offset E_m and the sliding base X_b. The coordinate system $S_s\{X_s, Y_s, Z_s\}$ is used to describe the machine root angle γ_m and the machine center to cross point X_p.

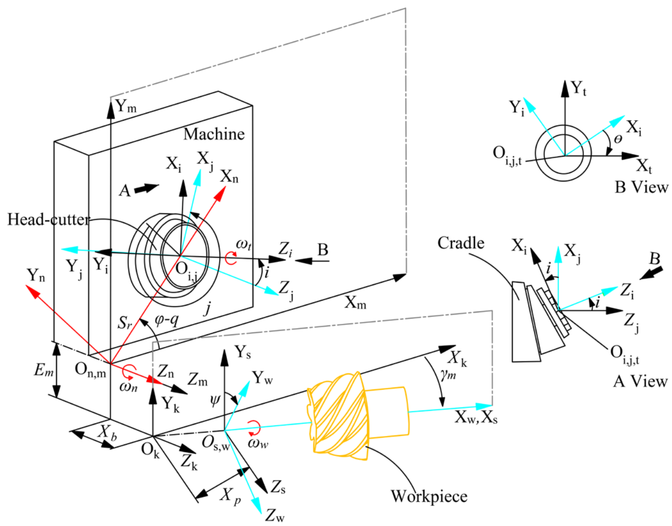

Fig. 1 Coordinate system applied for machining gear

From Figure 1, the model of the head-cutter's generated surface can be obtained, with the position vector extending from the head-cutter center to the cutter tip:

$$\mathbf{r}_0 = \begin{bmatrix} -\cos i \sin j \\ -\cos i \cos j \\ \sin i \end{bmatrix} \begin{bmatrix} 0 \\ -r_c \\ 0 \end{bmatrix}, \tag{1}$$

where $\mathbf{r}_c$ is the cutter point radius. The corresponding unit normal and tangential vectors of the gear generating surface can also be obtained as follows:

$$\mathbf{n}_0 = \begin{bmatrix} -\cos(\alpha_0 - i)\sin j \\ -\cos(\alpha_0 - i)\cos j \\ -\sin(\alpha_0 - i) \end{bmatrix}, \tag{2}$$

$$\mathbf{t}_0 = \begin{bmatrix} -\sin(\alpha_0 - i)\sin j \\ -\sin(\alpha_0 - i)\cos j \\ \cos(\alpha_0 - i) \end{bmatrix}. \tag{3}$$

Here, α_0 is the blade angle. After rotating the position vector, unit normal vector, and tangential vector of the generating gear by an arbitrary angle θ around the head-cutter axis Z_t, and then rotating the head-cutter by an angle q around the generating gear axis Z_m, these vectors can be expressed within the coordinate system S_m.

$$\mathbf{r}_1 = \mathbf{R}[\mathbf{c},\theta]\cdot\mathbf{R}[\mathbf{z},-q]\cdot\mathbf{r}_0 + S_r[\cos q \quad \sin q \quad 0]^{\mathrm{T}} + s\mathbf{t}_1, \tag{4}$$

$$\mathbf{n}_1 = \mathbf{R}[\mathbf{c},\theta]\cdot\mathbf{R}[\mathbf{z},-q]\cdot\mathbf{n}_0, \tag{5}$$

$$\mathbf{t}_1 = \mathbf{R}[\mathbf{c},\theta]\cdot\mathbf{R}[\mathbf{z},-q]\cdot\mathbf{t}_0. \tag{6}$$

Here, $\mathbf{c}$ is the unit vector of the cutter axis, $\mathbf{c} = [\sin I_1 \sin(q_1 - J_1) \quad -\sin I_1 \cos(q_1 - J_1) \quad -\cos I_1]^{\mathrm{T}}$, and s is the cutter profile parameter. $\mathbf{R}$ is the rotation matrix, as detailed in [28,29]. Assuming the angular velocity of the generating gear is 1, its vector can be expressed as follows $\boldsymbol{\omega}_p = [0 \quad 0 \quad 1]^{\mathrm{T}}$. The angular velocity vector of the pinion is $\boldsymbol{\omega}_1 = R_{a1}\mathbf{p}$, where R_{a1} is the roll ratio used to generate the pinion. $\mathbf{p} = [-\cos\gamma_m \ 0 \ \sin\gamma_m]^{\mathrm{T}}$ is the unit vector of the pinion axis. The relative angular velocity and relative linear velocity between the generating gear and the workpiece are expressed as follows:

$$\boldsymbol{\omega}_{p1} = \boldsymbol{\omega}_p - R_{a1}\mathbf{p}, \tag{7}$$

$$\mathbf{v}_{p1} = \boldsymbol{\omega}_{p1} \times \mathbf{r}_1 - R_{a1}\mathbf{p} \times \mathbf{m} + H[0,0,1]^{\mathrm{T}}, \tag{8}$$

where the position vector from the pinion crossing point O_w to the center of the machine O_m can be expressed as:

$$\mathbf{m} = X_b[0 \quad 0 \quad 1]^{\mathrm{T}} + X_p[-\cos\gamma_m \quad 0 \quad \sin\gamma_m]^{\mathrm{T}} - E_m[0 \quad 1 \quad 0]^{\mathrm{T}} \tag{9}$$

Substitute Eqs. (8) and (5) into the meshing equation $\mathbf{v}_{p1}\cdot\mathbf{n}_1 = 0$. By specifying a position on the tooth projection plane (two scalar values), three unknown variables among the vectors mentioned above (s, θ, q) can be determined. Finally, by expressing the arbitrary position vector of the generating gear in the pinion coordinate system S_w, the position vector of any point on the pinion tooth surface can be obtained.

$$\mathbf{r}_2 = \mathbf{r}_1 + \mathbf{m}. \tag{10}$$

2.2 Design Method for Gear Tooth Differential Modification

In the design of spiral bevel and hypoid gears, modifications are generally made to the pinion to improve processing efficiency. Therefore, this paper primarily focuses on the differential modification (DM) design of the pinion. DM refers to the method of using preset MP – the bias factor and profile separation factor – where the bias factor controls the inclination direction of the contact path on the tooth surface, and the profile separation factor controls the mismatch amount in the profile direction. These MP are varied according to a certain pattern (such as a sine function). This approach enables the DM design of the pinion tooth surface, aiming to balance in the fluctuations generated during gear transmission through the DM of adjacent teeth, thereby reducing gear vibration and noise. Figure 2 shows a schematic diagram of how the pinion's MP varies according to a sinusoidal function. The MP for each tooth is represented by z discrete values, with denoting the pinion tooth count.

By setting the amplitude of the modification parameter variation to A, the modification parameter θ_k for each tooth of the pinion can be determined by the following equation.

$$\theta_k = \theta_0 + \frac{A}{2}\sin\left(2\frac{\pi}{z}k\right). \tag{11}$$

Here, θ_0 represents the initial value of the preset MP for the pinion. The variable k denotes the current tooth number, with teeth numbered sequentially starting from 1.

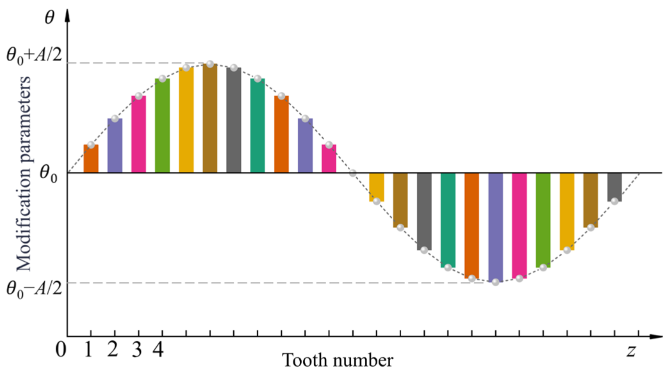

Fig. 2. Diagram of MP varying according to a sine function pattern

Taking a pair of hypoid gears 7×43 as an example, a DM design is performed on their tooth surfaces, and a simulation analysis of gear transmission performance is conducted. The geometric parameters and the basic machine settings without DM (with a corresponding bias factor and profile separation factor of 40 and 20, respectively) are listed in Tables 1 and 2. After DM implementation, each tooth possesses unique preset MPs, corresponding to distinct machine settings. Therefore, the topography of each tooth surface exhibits differences. For details regarding the optimization of machine settings for spiral bevel and hypoid gears, please refer to reference [7].

Table 1. Geometric parameters

Parameters	Pinion	Gear
Number of teeth	7	43
Module [mm]	6.861	-
Face width [mm]	43.6429	40.00
Pinion offset [mm]	25.40	-
Shaft angle [°]	90	-
Mean spiral angle [°]	49.9999	38.7715
Mean cone distance [°]	129.99695	130.4837
Pitch diameter [mm]	58.9784	295.0230
Hand of spiral	LH	RH
Cutting method	DUPLEX	FORMATE
Pitch angle [°]	11.2003	78.5868
Face angle [°]	14.2983	79.6361
Root angle [°]	10.1700	75.4337

The initial value of the bias factor is 40, with a variation amplitude of 0.05. The initial value of the profile separation factor is 20, also set with a variation amplitude of 0.05. The variation values of the bias factor and profile separation factor for the 7 teeth of the pinion, which follow a sine function pattern, are shown in Table 3. To more clearly compare the changes in the topography of each tooth surface after DM, a comparative analysis is conducted. Using a single-factor analysis method, the concave and convex surfaces of the pinion are compared by varying only the bias factor (keeping the profile separation factor constant at 20) and varying only the profile separation factor (keeping the bias factor constant at 40), as shown in Figs. 3 and 4.

Table 2. **Basic machine settings**

Parameters	Pinion	Gear
Cutter diameter [mm]	229.9257	228.60
Outside blade angle [°]	20.00	15.00
Inside blade angle [°]	25.00	30.00
Point width [mm]	3.0084	2.7940
Radial distance [mm]	109.23092	108.07168
Tilt angle [°]	16.07333	-
Swivel angle [°]	338.47262	-
Work offset [mm]	27.65168	-
Machine root angle [mm]	354.10339	70.21411
Machine center to cross point [mm]	0.90602	9.76886
Sliding base [mm]	11.81285	-
Ratio of roll	6.172925	-
Center roll position [°]	67.55503	71.65167
Helical motion velocity coefficient [mm/rad]	8.565421	-

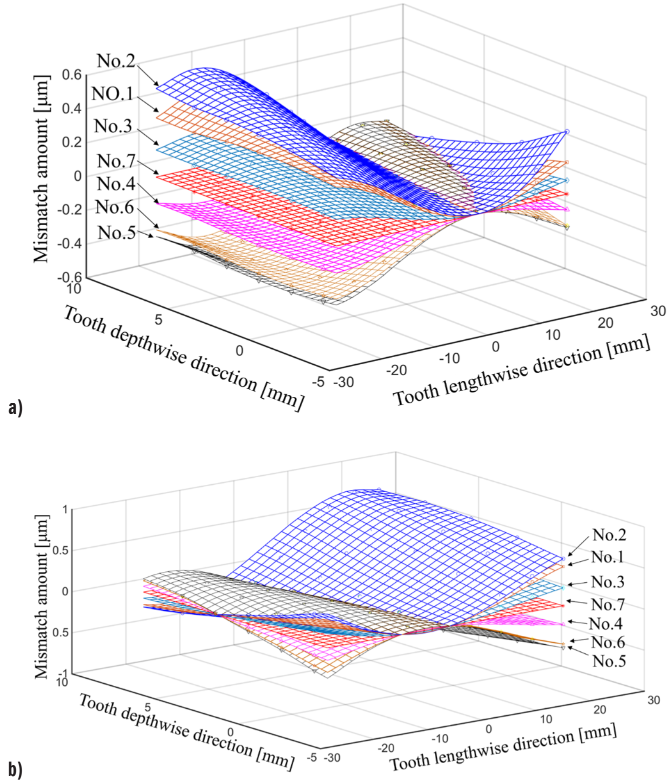

Fig. 3. **Comparison of topography of pinion tooth surfaces with changes in bias factor; a) pinion concave surfaces, and b) pinion convex surfaces**

From Figures 3 and 4, it can be seen that the bias factor affects the diagonal modification extent of the tooth surface topography. Generally, the larger the bias factor, the greater the mismatch in the diagonal direction, and the larger the inclination angle of the tooth surface contact path. The profile separation factor affects the modification magnitude of the tooth surface, the larger the profile separation factor, the greater the mismatch amount of the tooth surface. These observations confirm the correctness of the established model is correct when the hypoid gear pair is designed using the DM method based on MP, with the modification of each tooth surface exhibiting a sinusoidal pattern of change.

Table 3. **Pinion modification parameter sinusoidal settings**

Tooth serial number	Profile separation factor	Bias factor
1	20.039092	40.039092
2	20.048746	40.048746
3	20.021694	40.021694
4	19.978306	39.978306
5	19.951254	39.951254
6	19.960908	39.960908
7	20	40

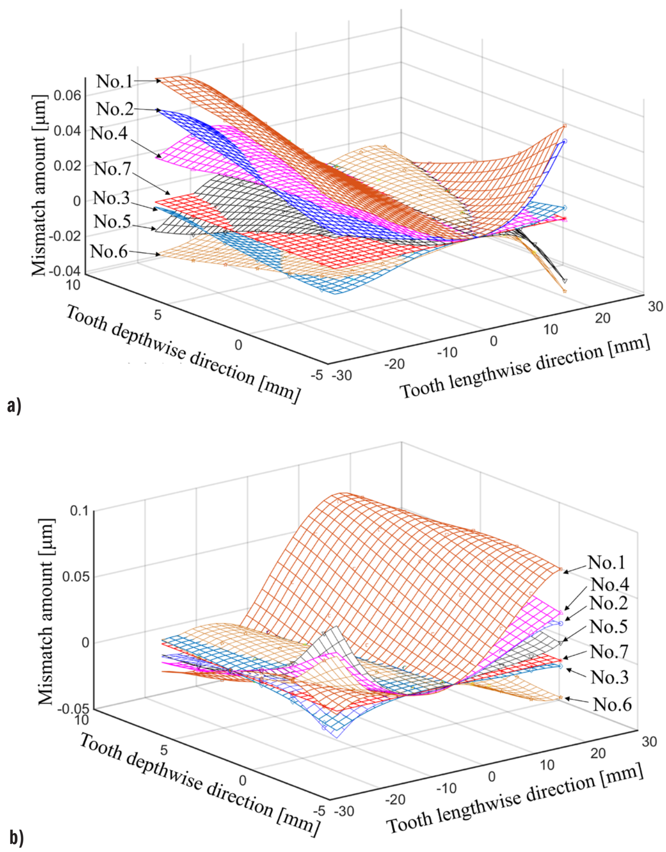

Fig. 4. **Comparison of topography of pinion tooth surfaces with changes in profile separation factor; a) pinion concave surfaces, and b) pinion convex surfaces**

2.3 Simulation Model of Gear Pair Dynamics

In the simulation process, the DM model of hypoid gear tooth surfaces requires a high-precision representation. Therefore, the mathematical model of the hypoid gear established in Subsection 3.1 is used to develop a high-precision dynamical model through secondary development method using Adams software, ensuring the accuracy of the simulation results. The specific gear parameters are detailed in Table 1. As shown in Fig. 5, the constructed dynamic simulation model of the hypoid gear pair uses 45# steel as the gear material, with a Poisson's ratio of 0.3, a Young's modulus of 210 GPa, and a density of 786 kg/m³. Rotational motion pairs are added to the axes of the gear and pinion, and the contact force between the tooth surfaces is set using the impact function for collision contact, with the contact type being solid-to-solid. The contact and material parameters are detailed in Table 4. A step function is used to define the driving speed of the pinion, accelerating to the predetermined operating speed within 0 to 0.1 seconds, while the driven gear is subjected to a torque load corresponding to the predetermined operating load, maintaining these conditions from 0.1 s to 0.5 s. As shown in Fig. 5a, after obtaining the spatial coordinates of discrete tooth surface points, the three-dimensional solid model of the hypoid gears can be constructed based on these data. The final dynamic model of the hypoid gear is shown in Fig. 5b.

Table 4. Parameters setting

Parameter	Value
Stiffness [N/mm]	150900
Static friction coefficient	0.3
Force exponent	1.6
Static displacement coefficient [mm/s]	100
Damping [N·s/mm]	10
Dynamic friction coefficient	0.1
Penetration depth [mm]	0.1
Frictional displacement coefficient [mm/s]	1000

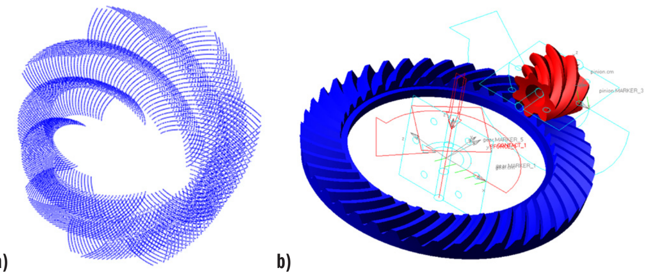

a) b)

Fig. 5. Establishment of gear pair dynamic model; a) tooth surface discrete points, and b) dynamic model

3 RESULTS AND DISCUSSION

3.1 Analysis of Meshing Force and Angular Acceleration with Sine-Wave-Based Bias Factor

The variation in angular acceleration and meshing force during gear transmission are key indicators reflecting the dynamic meshing performance of gear pairs, directly related to gear vibration and noise

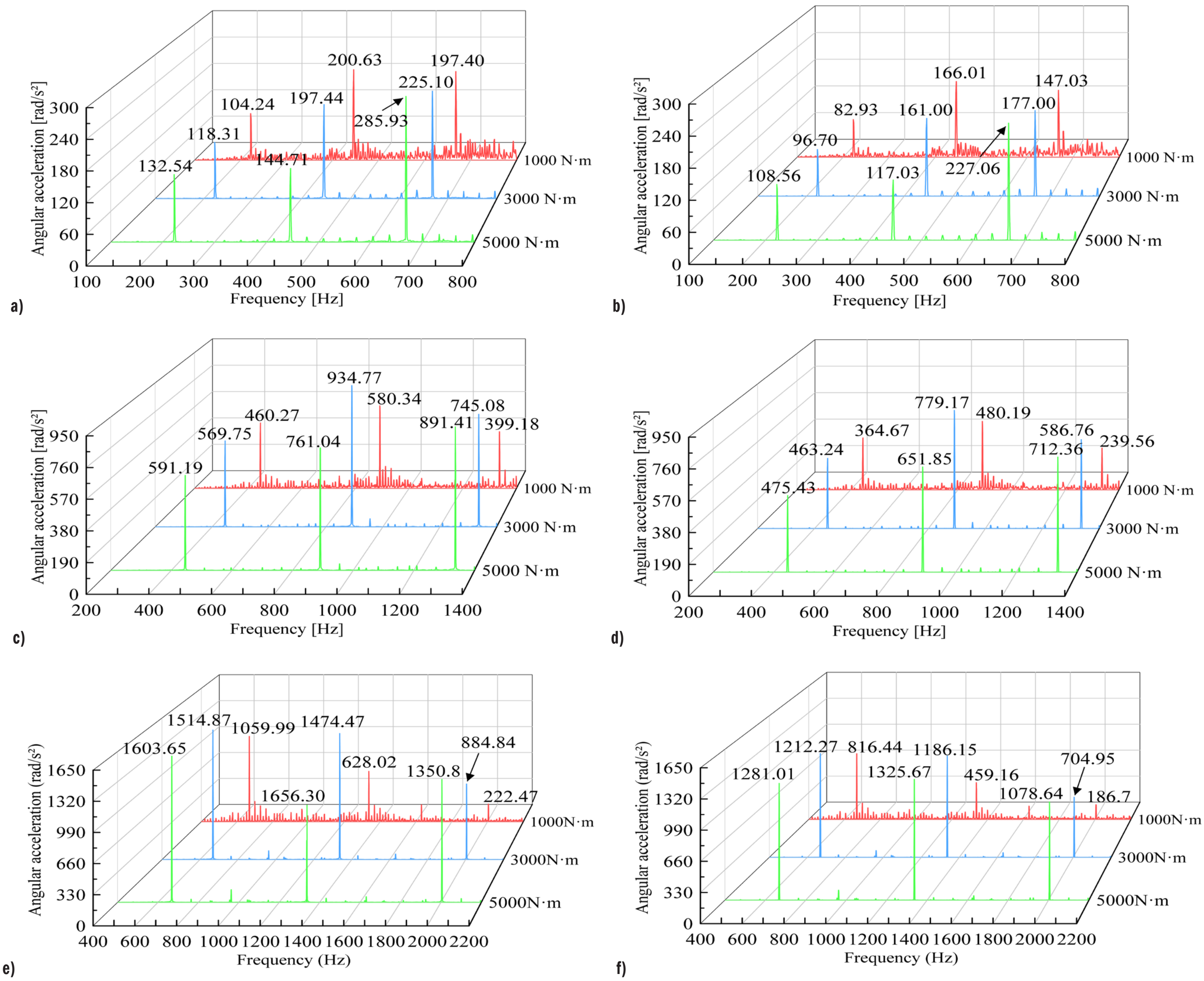

Fig. 6. Comparison of angular acceleration spectrum between TM and SWB design gear pairs of bias factor; a) TM at 200 rad/s, b) SWB at 200 rad/s, c) TM at 400 rad/s, d) SWB at 400 rad/s, e) TM at 600 rad/s, and f) SWB at 600 rad/s

[30-33]. Therefore, by comparing the normally designed hypoid gear pairs with the DM-designed gear pairs using Adams software, the transmission performance can be evaluated in terms of the meshing force and angular acceleration. Three load conditions of 1000 Nm, 3000 Nm, and 5000 Nm are set at the output end of the gear, and three common rotational speeds of 200 rad/s, 400 rad/s, and 600 rad/s are set at the input end of the pinion. The meshing performance of the gear pairs under different loads and angular velocities is studied to verify the feasibility of improving the transmission performance of gear pairs through the DM design method.

Figure 6 shows the angular acceleration curves of the gear under various conditions for gear pairs using the TM method and those with sine-wave-based (SWB) bias factors. It compares the reduction in amplitude of the first three orders of meshing harmonics between the two methods. From the comparative analysis, it can be concluded that:

1. When the rotational speeds are 200 rad/s, 400 rad/s, and 600 rad/s, the theoretical meshing frequencies are 222.82 Hz, 445.63 Hz, and 668.45 Hz, respectively, according to the meshing frequency calculation formula. The frequency of the first peak in the figures is generally consistent with the gear pair meshing frequency. During meshing, dominant spectral peaks appear at integer multiples of the meshing frequency, verifying the correctness of the gear transmission model.
2. At a constant rotational speed, as the load increases, the peak value of angular acceleration at meshing harmonics shows an upward trend. At the same load, as the rotational speed increases, the peak value of angular acceleration at meshing harmonics also increases significantly, indicating that both rotational speed and load are influencing factors for angular acceleration, but rotational speed exerts a greater impact.
3. In 9 conditions and 27 harmonics, compared to gear pairs designed with the TM method, all meshing harmonic amplitudes of gear pairs with SWB bias coefficient design are reduced. This fully demonstrates the feasibility of using DM methods to achieve vibration and noise reduction. The minimum observed reduction in angular acceleration is 14.35 %, and the maximum reduction is 39.99 %.
4. Overall, the gear pairs designed with the DM method show better transmission performance under all conditions. Moreover, as the rotational speed increases, the reduction in the amplitude of angular acceleration frequency becomes more pronounced.

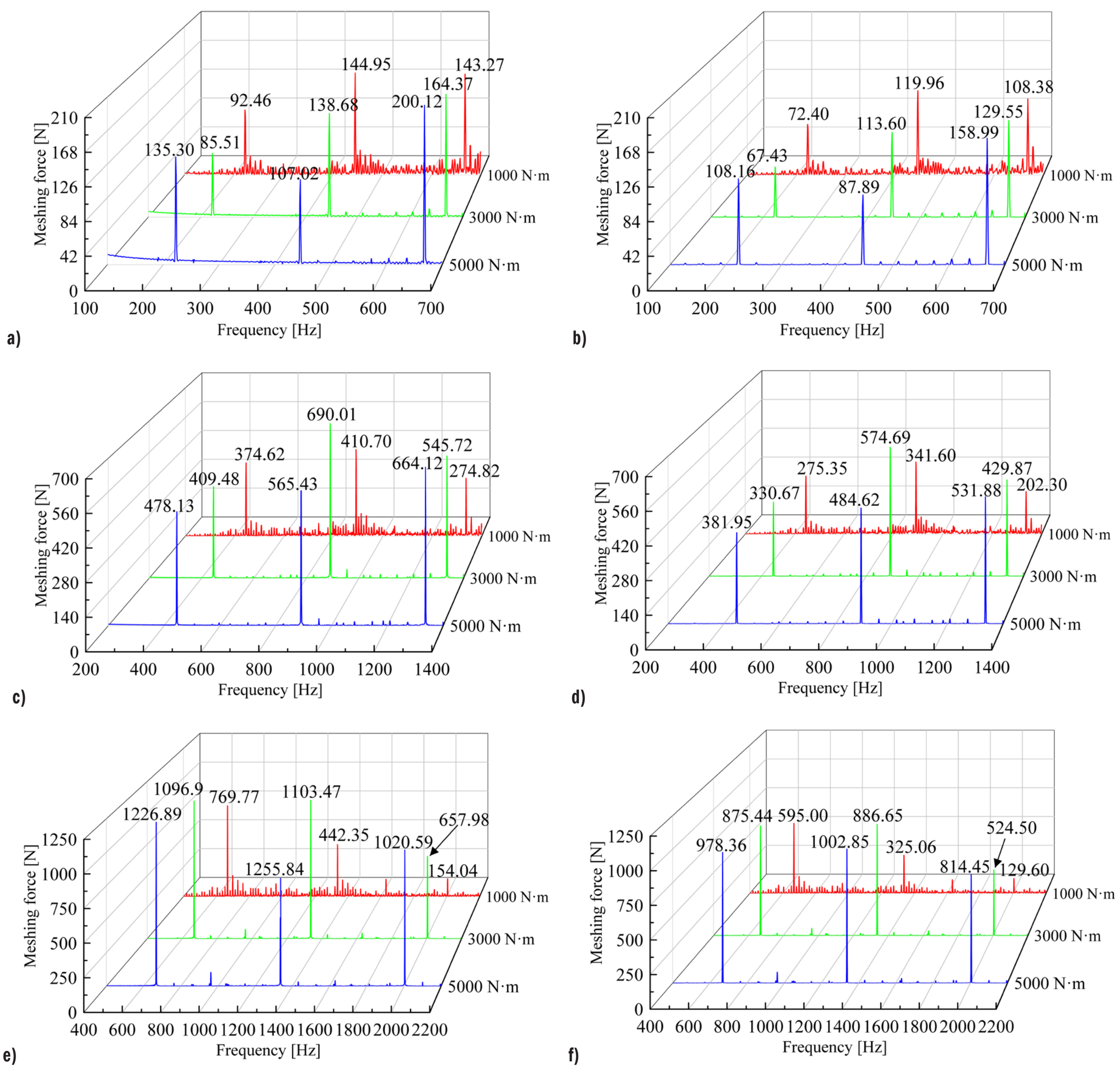

Fig. 7. Comparison of meshing force spectrum between TM and SWB design gear pair of bias factor;
a) TM at 200 rad/s, b) SWB at 200 rad/s, c) TM at 400 rad/s, d) SWB at 400 rad/s, e) TM at 600 rad/s, and f) SWB at 600 rad/s

Figure 7 shows the frequency spectrum of meshing forces under various conditions for gear pairs designed using the TM method and the bias factor SWB design. By comparing the reduction in amplitude of the first three harmonics of meshing frequencies between the SWB and TM designs, the following conclusions can be drawn from the analysis and comparison of these figures:

1. Under 9 operating conditions and across 27 harmonics, gear pairs designed using the SWB bias factor method show a significant reduction in the amplitude of meshing force harmonics compared to those designed with the TM method. This further validates the feasibility of the DM method for gear teeth. The minimum reduction in frequency amplitude of the meshing force is 16.67 %, and the maximum is 36.08 %.
2. Under the same rotational speed conditions, two of the first three harmonics at a load condition of 1000 Nm show better reduction effects compared to the corresponding harmonics at other load conditions, and this pattern does not change with increasing rotational speed. Overall, as both rotational speed and load increase, the reduction in meshing force frequency amplitude becomes more stable for gear pairs designed with the SWB bias factor method.
3. The frequency-domain characteristics of meshing forces were analyzed and compared with angular acceleration patterns. Both parameters exhibited similar variation trends across operational conditions. This correlation confirms that both parameters are reliable and consistent evaluation metrics.

3.2 Analysis of Meshing Force and Angular Acceleration with SWB Profile Separation Factor

Employing the same analytical approach used for the SWB bias factor design, a comparative analysis was conducted between gear pairs designed using the SWB profile separation factor and those designed using the TM method. Under different operating conditions, the frequency domain diagram of the angular acceleration for gear pairs with the SWB profile separation factor design is shown in Fig. 8. This is compared with the frequency domain diagrams of angular acceleration for gear pairs designed using the TM method (Figs. 6a, c and e). The following conclusions can be drawn from the analysis and comparison of the figures:

1. At the same rotational speed, as the load increases, the amplitude of the angular acceleration harmonics gradually increases. At the same load, as the rotational speed increases, the frequency amplitude of the angular acceleration also increases significantly.
2. At 200 rad/s, TM-designed pairs exhibit higher amplitudes than SWB.
3. In 23 out of 27 operating conditions, the SWB profile separation factor design shows a reduction in harmonic amplitudes compared

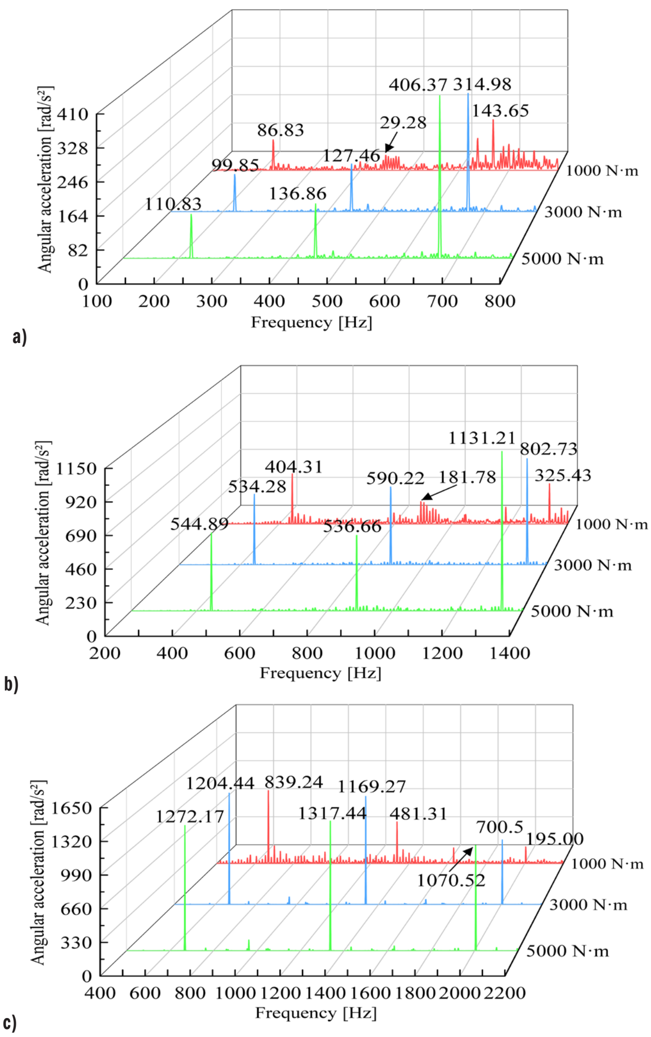

Fig. 8 Angular acceleration spectrum with SWB design of profile separation factor at; a) 200 rad/s, b) 400 rad/s, c) 600 rad/s

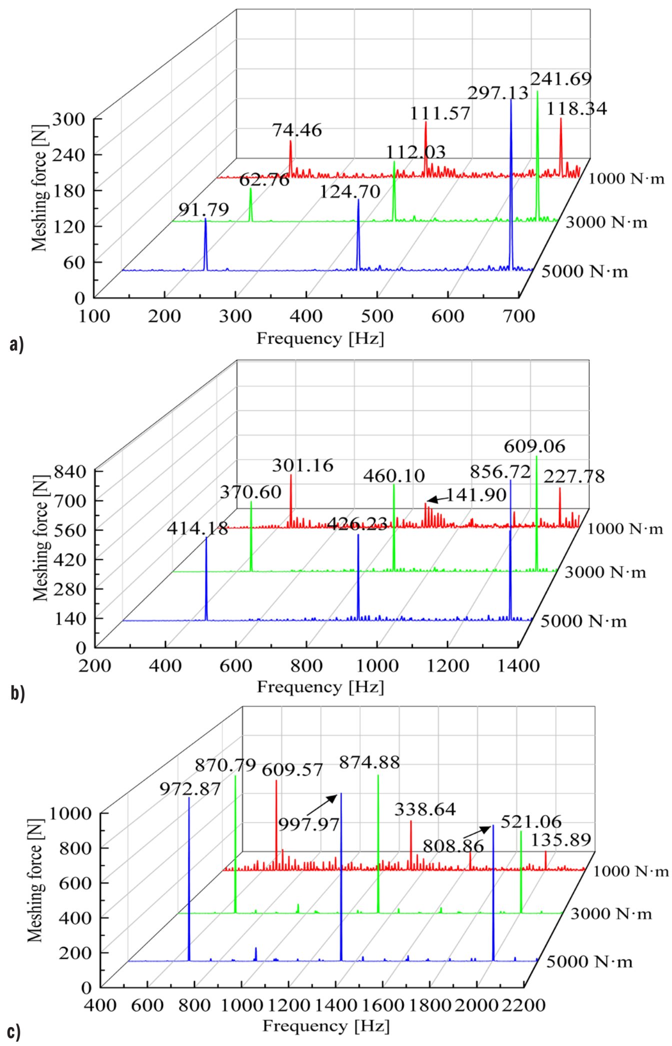

Fig. 9. Meshing force spectrum with SWB design of profile separation factor at; a) 200 rad/s, b) 400 rad/s, c) 600 rad/s

to the TM method. The maximum reduction in the first harmonic amplitude occurs at a load of 5000 Nm and a rotational speed of 600 rad/s, reaching 20.67 %. The maximum reduction in the second harmonic amplitude occurs at a load of 1000 Nm and a rotational speed of 200 rad/s, reaching 85.41 %. The maximum reduction in the third harmonic amplitude occurs at a load of 1000 Nm and a rotational speed of 200 rad/s, reaching 27.23 %.
4. Compared to the TM method, the SWB profile separation factor design significantly reduces the amplitude of the second harmonic at medium and low rotational speeds and low loads. As the rotational speed increases, the reduction effect on the second harmonic amplitude gradually weakens. However, at 600 rad/s, stable reductions occur across all harmonics.

Figure 9 shows meshing force spectra for SWB-designed gear pairs. It highlights the reduction in the amplitude of the first three harmonics of the meshing force compared to gear pairs designed using the TM method. From the comparative analysis of the figures, the following conclusions can be drawn:
1. The gear pairs designed with the SWB profile separation factor were analyzed at rotational speeds of 200 rad/s and 400 rad/s. Compared to the TM method design, the SWB-based pairs exhibited reduced amplitude in the second harmonic of meshing force. Notably, the amplitude reduction in the third harmonic showed a slight improvement under these conditions. The reduction pattern of the meshing force harmonics is consistent with that of the angular acceleration harmonics.
2. At the same rotational speed, the gear pairs designed with the SWB profile separation factor can achieve a significant reduction in the second harmonic amplitude of the meshing force under a load of 1000 Nm compared to those designed with the TM method. However, as the load increases, this effect gradually declines.
3. Overall, compared to gear pairs designed with the TM method, gear pairs designed with the SWB profile separation factor achieve a reduction in amplitude for 81.48% of the harmonics, with the minimum reduction being 9.49% and the maximum reduction being 65.45 %. Under specific operating conditions, SWB profile separation factor design outperforms SWB bias factor designs.

4 CONCLUSIONS

The simulation study on the dynamic meshing performance of gear pairs was conducted based on the DM method for the tooth surfaces of spiral bevel and hypoid gears. The main conclusions are as follows:
1. A DM method was proposed, in which the MP -– bias factor and profile separation factor – of spiral bevel and hypoid gears were set according to a sinusoidal function. The impact of sinusoidal settings of these two MP on the topography of each tooth surface was analyzed.
2. A mathematical model of the spiral bevel and hypoid gears was established, and a dynamic model was developed using the secondary development method based on Adams software. The effectiveness of the DM method for spiral bevel and hypoid gear tooth surfaces was verified through simulation and analysis using a representative pair of hypoid gears as an example.
3. Compared to the TM method, the DM method using a SWB design of the bias factor showed a decreasing trend in the amplitude of the first three harmonics under various working conditions. The maximum reduction in the first harmonic amplitude of the angular acceleration and meshing force reached 22.98 % and 36.05 %, respectively.
4. Compared to gear pairs using the TM method, those designed with a SWB profile separation factor achieved a reduction in the amplitude of the first three harmonics of angular acceleration and meshing force under most working conditions. In some cases, the amplitude of the third harmonic increased slightly. However, at a rotational speed of 600 rad/s, the amplitude of all harmonic frequencies effectively decreased. The maximum reduction in the first harmonic amplitude of the angular acceleration and meshing force reached 20.83 % and 32.16 %, respectively.
5. The simulation results demonstrated that the DM design method for tooth surfaces can effectively reduce angular acceleration and meshing force, providing a new approach to suppress gear vibration and noise.
6. The gear differential design method offers and will provide new insights for future research on vibration and noise reduction strategies in high-speed gears. This approach will further integrate with disciplines such as psychoacoustics and signal detection, offering more innovative solutions for high-performance gear design. However, the implementation of gear differential design will also pose new challenges for gear measurement technology.

Nomenclature

rc	cutter point radius, [mm]
α_0	blade angle, [º]
θ	cutter head's rotation angle, [º]
j	cutter swivel angle, [º]
S_r	radial distance,[mm]
i	cutter tilt angle, [º]
E_m	work offset, [mm]
X_b	sliding base, [mm]
γ_m	machine root angle, [º]
X_p	machine center to cross point, [mm]
c	unit vector of the cutter axis
s	cutter profile parameter, [mm]
$\mathbf{R}$	rotation matrix
z	number of teeth on the pinion
A	amplitude
θ_k	modification parameter
θ_0	initial value of the preset MP
k	current tooth number
R_{a1}	Roll ratio when generating the pinion
$\boldsymbol{\omega}_p$	Angular velocity vector of the generating gear, [rad/s]
$\boldsymbol{\omega}_1$	angular velocity vector of the pinion, [rad/s]
$\mathbf{p}$	unit vector of the pinion axis
$\boldsymbol{\omega}_{p1}$	Relative angular velocity between the generating gear and the workpiece, [rad/s]
$\mathbf{v}_{p1}$	relative motion velocity between the generating gear and the workpiece, [mm/s]
$\mathbf{m}$	position vector from the pinion crossing point O_w to the center of the machine O_m, [mm]
H	Helical motion velocity coefficient [mm/rad]

References

[1] Stadtfeld, H.J. Automotive drive concepts. *Gear Tech* 66-73 (2020).
[2] Stadtfeld, H.J. Introduction to electric vehicle transmissions. *Gear Tech* 42-50 (2020).
[3] Stadtfeld, H.J. Psychoacoustics Applied to eDrive Noise Reduction. *Gear Tech* 72-78 (2021).
[4] Stadtfeld, H.J. *eDrive Transmission Guide. New Solutions for Electric and Hybrid Vehicle Transmissions*. The Gleason Works, Rochester, New York (2020).
[5] Cattanei, A., Ghio, R., Bongiovì, A. Reduction of the tonal noise annoyance of axial flow fans by means of optimal blade spacing. *Appl Acoust* 68 1323-1345 (2007) **DOI:10.1016/j.apacoust.2006.07.012**.
[6] Stadtfeld, H.J. Gleason bevel gear technology. The Gleason Works, Rochester (2014) **DOI:10.36198/9783838551685**.
[7] Zhang, Y., Yang, H. New methodology for determining basic machine settings of spiral bevel and hypoid gears manufactured by duplex helical method. *Mech Mach Theory* 100 283-295 (2016) **DOI:10.1016/j.mechmachtheory.2016.02.015**.
[8] Stadtfeld, H.J. *Practical Gear Engineering: Answers to Common Gear Manufacturing Questions*. The Gleason Works, Rochester (2019).
[9] Mu, Y., Fang, Z., Li, W. Impact analysis and vibration reduction design of spiral bevel gears. *P I Mech Eng K-J Mul* 233 668-676 (2019) **DOI:10.1177/1464419319827398**.

[10] Mu, Y., Li, W., Fang, Z., Zhang, X. A novel tooth surface modification method for spiral bevel gears with higher-order transmission error. *Mech Mach Theory* 126 49-60 (2018) **DOI:10.1016/j.mechmachtheory.2018.04.001**.

[11] Mu, Y., Li, W., Fang, Z. Tooth surface modification method of face-milling spiral bevel gears with high contact ratio based on cutter blade profile correction. *Int J Adv Manuf Tech* 106 3229-3237 (2020) **DOI:10.1007/s00170-019-04738-3**.

[12] Samani, F.S., Molaie, M., Pellicano, F. Nonlinear vibration of the spiral bevel gear with a novel tooth surface modification method. *Meccanica* 54 1071-1081 (2019) **DOI:10.1007/s11012-019-00973-w**.

[13] Chen, P., Li, B., Wang, S.-M. A novel design method of low noise spiral bevel gear tooth surface for polynomial ease-off topological modification. *P I Mech Eng E-J Pro* 239 1364-1377 (2023) **DOI:10.1177/09544089231191370**.

[14] Nie, S., Chen, J., Liu, S. Research on noise reduction of drive axle hypoid gear based on tooth surface mismatch modification. *Adv Mech Eng* 16 (2024) **DOI:10.1177/16878132241228195**.

[15] Lin, C.-C. *Hypoid Gear Noise and Vibration Control in Automotive Rear Axle Systems*. PhD Thesis, University of Texas at Arlington, Arlington (2020).

[16] Chen, S., Wang, L., Fan, L., Lu, C., Xiao, Z. Nonlinear correction of hypoid gear machine tool parameters by duplex helical method. *J Mech Sci Technol* 38 6847-6857 (2024) **DOI:10.1007/s12206-024-1136-3**.

[17] Tian, X., Sun, Y., Mu, W., Xia, L., Han, J. High-Speed and Low-Noise Gear Finishing by Gear Grinding and Honing: A Review. *Chin J Mech Eng* 37 127 (2024) **DOI:10.1186/s10033-024-01078-6**.

[18] Hou, L., Lei, Y., Fu, Y., Hu, J. Effects of lightweight gear blank on noise, vibration and harshness for electric drive system in electric vehicles. *P I Mech Eng K-J Mul* 234 447-464 (2020) **DOI:10.1177/1464419320915006**.

[19] Cai, Z.-J., Zheng, X.-Q., Lan, H.-Q., Wang, L.-N., Yang, S.-W., Sheng, R. Time-Varying Meshing Stiffness and Dynamic Parameter Model of Spiral Bevel Gears with Different Surface Roughness. *Appl Sci-Basel* 14 1533 (2024) **DOI:10.3390/app14041533**.

[20] Lin, Z., Yao, L., Zhang, J., Su, T., Chen, K. Tooth contact analysis with latent error of double circular-arc spiral bevel gears for industrial robot joint nutation drive. *J Braz Soc Mech Sci* 42 10 (2020) **DOI:10.1007/s40430-019-2085-0**.

[21] Zhu, H., Chen, W., Zhu, R., Zhang, L., Fu, B., Lu, X. Modeling and dynamic analysis of spiral bevel gear coupled system of intermediate and tail gearboxes in a helicopter. *P I Mech Eng C-J Mec* 235 5975-5993 (2021) **DOI:10.1177/0954406221992798**.

[22] Sun, B., Liu, H., Tang, J., Rong, S., Liu, Y., Jiang, W. Optimization of heat treatment deformation control process parameters for face-hobbed hypoid gear using FEA-PSO-BP method. *J Manuf Process* 117 40-58 (2024) **DOI:10.1016/j.jmapro.2024.02.025**.

[23] Bozca, M. Transmission error model-based optimisation of the geometric design parameters of an automotive transmission gearbox to reduce gear-rattle noise. *Appl Acoust* 130 247-259 (2018) **DOI:10.1016/j.apacoust.2017.10.005**.

[24] Bozca, M. Torsional vibration model based optimization of gearbox geometric design parameters to reduce rattle noise in an automotive transmission. *Mech Mach Theory* 45 1583-1598 (2010) **DOI:10.1016/j.mechmachtheory.2010.06.014**.

[25] Qi, L., Zhou, J., Jin, P., Wang, M., Su, Y., Zhou, H., et al. Low noise optimization of two-stage gearbox housing structure based on acoustic contribution analysis and topology optimization. *J Mech Sci Technol* 37 4533-4544 (2023) **DOI:10.1007/s12206-023-0810-1**.

[26] Anuradha, G., Sagi, R.P., Shakya, P., Sekhar, A.S. Influence of Geometric Parameters on the Dynamic Performance of Spiral Bevel Gear. *J Vib Eng Technol* 12 9097-9111 (2024) **DOI:10.1007/s42417-024-01327-x**.

[27] Fastl, H., Zwicker, E. *Psychoacoustics*. Springer, Berlin (2007) **DOI:10.1007/978-3-540-68888-4**.

[28] Zhang, Y., Yan, H.Z., Zeng, T. Design and Manufacture of Spiral Bevel and Hypoid Gears by Duplex Helical Method. Central South University Press, Changsha (2021).

[29] Litvin, F.L., Fuentes, A. Gear Geometry and Applied Theory. Cambridge University Press, New York (2004) **DOI:10.1017/CBO9780511547126**.

[30] Xia, Y., Pang, J. Investigation on vibro-impacts of driveline system based on a nonlinear clearance element with time-varying stiffness and oil-squeeze damping. *J Vib Acoust* 144 031014 (2022) **DOI:10.1115/1.4053477**.

[31] Wang, L., Wu, X., Zhang, W. Applied research of the multi-stage torsional vibration damper on controlling the gear rattle. *J Virboeng* 18 4550-4562 (2016) **DOI:10.21595/jve.2016.17722**.

[32] Dai, H., Long, X., Chen, F., Bian, J. Experimental investigation of the ring-planet gear meshing forces identification. *J Sound Vib* 493 115844 (2021) **DOI:10.1016/j.jsv.2020.115844**.

[33] Xu, B., Qiu, Y., Yin, B., Hua, X., Du, H. Influence of Different Modified Gears on the Vibration and Noise of Electric Vehicle Reducer. *Int J Acoust Vib* 26 325-336 (2021) **DOI:10.20855/ijav.2021.26.41824**.

Received: 2024-12-20, Revised: 2025-05-27, Accepted: 2025-06-17 *as Original Scientific Paper.*

Acknowledgments *The research was supported by the Natural Science Foundation of Hunan Province (2024JJ5643), the National Natural Science Foundation of China (U22B2084 and 52475055), the Hunan Provincial Key R&D Program (2023GK2053).*

Data availability *The data supporting the findings of this study are included in the article and/or its supplementary materials.*

Author contribution *Yu Zhan: Methodology and Project administration, Chengyu Duan: Writing - original draft, Xiao Li: Investigation and Software, Zhiyong Wang: Validation, Yanli Ma: Formal analysis, Guoqi He: Visualization.*

Metoda diferencialne modifikacije površin za zmanjšanje vibracij v spiralnih stožčastih in hipoidnih zobnikih

Povzetek *Za obravnavo problema povečanega hrupa zobnikov v pogonih električnih vozil zaradi višjih vrtilnih hitrosti je predlagana metoda diferencialne modifikacije zobnih površin za spiralne stožčaste in hipoidne zobnike. Z vektorsko metodo je oblikovan matematični model spiralnih stožčastih in hipoidnih zobnikov. Na osnovi tega modela je bil s sekundarnim razvojem v programski opremi Adams razvit dinamični model zobnikov po metodi končnih elementov. Raziskana je metoda modifikacije zobne površine, kjer parametra (faktor odmika in faktor ločitve profila) variirata po sinusni funkciji, skupaj z njenim vplivom na mikrotopografijo zobne površine. Izvedena je bila primerjalna simulacijska analiza, s katero so ovrednotili metodo načrtovanja sinusnih parametrov v primerjavi s tradicionalnimi metodami modifikacij, s poudarkom na kotnem pospešku zobnika in sili v spregi pri različnih obratovalnih pogojih. Rezultati so pokazali, da diferencialna metoda modifikacije občutno zmanjša amplitude pri prvih treh redih spregnih frekvenc v skoraj vseh pogojih, pri čemer je doseženo največje zmanjšanje za 22,98 % in 36,05 % v amplitudah prvega reda frekvenc kotnega pospeška zobnika oziroma sile v spregi. To potrjuje učinkovitost metode pri zmanjševanju vibracij in hrupa zobnikov. Predlagana diferencialna metoda modifikacije spiralnih stožčastih in hipoidnih zobnikov tako predstavlja nov pristop k zmanjšanju vibracij in hrupa ter nudi dragoceno tehnično podporo pri načrtovanju in proizvodnji pogonov električnih vozil visoke zmogljivosti.*

Ključne besede *spiralni stožčasti in hipoidni zobniki, diferencialna modifikacija zobnih površin, dinamična simulacija, kotni pospešek, sila v spregi*